FEATURES EXTRACTION ON COMPLEX IMAGES

Pierrick Bourgeat[a,b], Fabrice Meriaudeau[a], Patrick Gorria[a], Kenneth W. Tobin[c], Frédéric Truchetet[a]

[a]Le2i Laboratory – University of Burgundy – France,
[b]BioMedIA Laboratory – CSIRO – Australia,
[c]Oak Ridge National Laboratory – USA.

ABSTRACT

In the last decade, the accessibility of inexpensive and powerful computers has allowed true digital holography to be used for industrial inspection using microscopy. This technique allows capturing a complex image of a scene (i.e. containing magnitude and phase), and reconstructing the phase and magnitude information. Digital holograms give a new dimension to texture analysis since the topology information can be used as an additional way to extract features. This new technique can be used to extend previous work on image segmentation of patterned wafers for defect detection. This paper presents a comparison between the features obtained using Gabor filtering on complex images under illumination and focus variations.

1. INTRODUCTION

In the last decade, the accessibility of inexpensive and powerful computers has allowed true digital holography to be used for industrial inspection using a microscopy. The Direct-to-Digital Holography (DDH) technique allows capturing a complex image of a scene, and reconstructing the phase and magnitude information [1]. The magnitude image corresponds to the information that can be captured with a classical microscope, and the phase image provides information about the topology of the scene. The combination of this data gives a complete 3D representation of the scene, within the wavelength depth of the laser used to produce the hologram. This type of image gives a new dimension to texture analysis, since the topology information can be used as an additional mechanism to extract features. This new technique can be used to extend our previous work [2, 3] on image segmentation of patterned wafers for defect detection.

In die-to-die wafer inspection [4], defect detection is based upon the comparison of the same area on two neighboring die. The dissimilarities between the images are a result of defects in the area of one of the die. The two images are subtracted, and a threshold level is selected to locate any anomaly. This threshold is established based upon the noise level in the difference image, to optimize the signal-to-noise ratio. The noise level can vary from one structure to the next, within the same image since multiple structures coexist in the same field of view. Therefore, the measure of noise within the whole image is not sufficient for each individual type of structure. Segmentation is needed to create a mask of these different regions. This mask is then used to produce a measure of noise for each structure in the difference image, leading to an individual threshold for each region. In our previous work, features for the segmentation were extracted using three levels of wavelet decomposition based on the "à trous" algorithm [5], with coifman wavelets coefficients. This produces a translation invariant set of features that are smoothed by the local estimate of the standard deviation in an M×N sliding window. A stress polytopes classifier [6] was used to segment the images. Process variations, focus changes and non-uniform illumination affect the texture of the recorded images and introduce contrast variations that change the response of some of the features. This increases the complexity in training the classifier since the whole range of variations needs to be included in the training set to achieve the best segmentation results, which presents a significant problem when dealing with large amounts of data. This point was addressed by using a technique to predict feature variations within a limited set of training samples and modify the classifier characteristics accordingly [2, 3]. The technique was proved to give good performance, but quickly reach a limit when the variations become larger. This statement leads us to investigate another set of feature extraction techniques based on Gabor filtering, with the SVM [7] classifier. Gabor filtering provides the ability to process complex images to generate features based on the phase and magnitude information.

2. DDH

Thomas, *et al* [1], developed a digital implementation of modern spatial heterodyne holography. A small angle between the object and the reference beam creates interfer-

ence fringes that carry the phase information. The Mach-Zehnder interferometer arrangement used is described in figure 1. The laser beam is divided by the beam splitter into the object beam and the reference beam. The object beam is reflected by the wafer surface, while the reference beam is reflected by a flat mirror, following an identical path. The beamsplitter in front of the camera mixes the two beams together with a small angle to create the interference fringes.

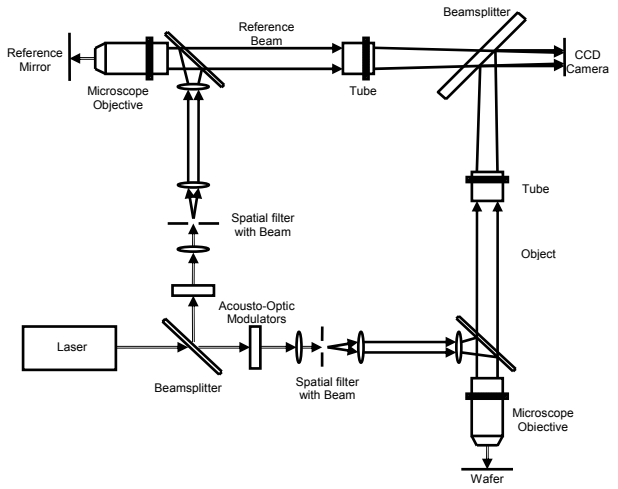

Figure 1. DDH interferometer

This technique allows recording of the complex wavefront, and reconstruction of the phase and magnitude information with a single image. The recorded hologram presents the interferometric fringes modulated by the phase information as shown in figure 2.

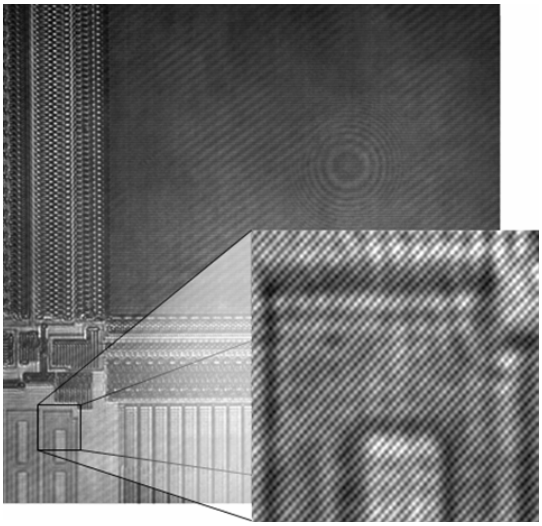

Figure 2. Hologram and the interference fringes

The reconstruction is performed by filtering in Fourier space. The Fourier transform of the hologram is composed of the central autocorrelation region containing the magnitude information, and the two complex conjugate sidebands that correspond to the complex wavefront information. One of the sidebands is extracted and centered, and lowpass filtered to remove the autocorrelation and the other sideband information. The complex image is generated with the inverse Fourier transform. By the end of the reconstruction process, a complex image is available, and can be processed using the phase and the magnitude information, or the real and imaginary information. After filtering, the complex image $I(x,y)$ can be expressed as:

$$I(x,y) = A(x,y) \cdot e^{j\varphi(x,y)}, \tag{1}$$

with $A(x,y)$ the amplitude image, and $\varphi(x,y)$ the phase image.

3. GABOR TRANSFORM ON COMPLEX IMAGES

The advantages of the phase image over the magnitude rely on the formation of those images. On one hand, the magnitude image is very sensitive to intensity variation on the wafer, to non-uniform illumination and more sensitive to noise in general. On the other hand, the phase image is not affected by color variation or non uniform illumination since it is a measure of the topography of the wafer that gives a greater immunity to noise. However, phase wraps constitute a major drawback that prevents the phase image from being directly used for segmentation. There have been several unwrapping algorithms developed [8], but they do not typically resolve abrupt height changes in the phase, and they are usually compute intensive.

Complex images are already available in interferometric synthetic aperture radar for topology estimation [9], but usually, only the amplitude of the signal is used for segmentation purposes. The phase image is difficult to extract, because two different images are required to obtain meaningful information. This phase image is also hardly usable for segmentation because of the issue of phase wraps.

With true holograms, since the complex information is contained in the original complex image (i.e., prior to unwrapping), it can be used directly to extract 3D information without dealing with phase unwrapping. With this type of information, features can be extracted using complex Gabor filtering [10, 11] in Fourier space. The features are then a representation of both the amplitude and the phase of the signal, thus containing more information than processing just the amplitude of the signal, or just the phase. The Gabor filters are defined by their impulse response $h(x, y)$:

$$h(x,y) = g(x,y)\exp\left[j2\pi(Ux+Vy)\right]. \tag{2}$$

with

$$g(x,y) = \frac{1}{2\pi\sigma_x\sigma_y}\exp\left\{-\frac{1}{2}\left[\left(\frac{x}{\sigma_x}\right)^2+\left(\frac{y}{\sigma_y}\right)^2\right]\right\}. \tag{3}$$

The $h(x, y)$ function is a complex sinusoid of frequency (U, V) with a gaussian envelop $g(x, y)$ of shape defined by (σ_x, σ_y). The Fourier transform of $h(x, y)$ is:

$$H(u,v) = G(u-U, v-V), \tag{4}$$

with

$$G(u,v) = \exp\left[-2\pi^2\sigma_x\sigma_y\left(u^2+v^2\right)\right], \tag{5}$$

the Fourier transform of $g(x, y)$. The Fourier transform of the input image is multiplied by H(u, v), and transformed back into spatial coordinates. The amplitude of the resulting image is directly used as a feature for the classifier. The bank of Gabor filters is oriented in the horizontal and vertical direction corresponding to the principal orientation of the structures on a semiconductor wafer. The filter bank layout is presented on figure 3.

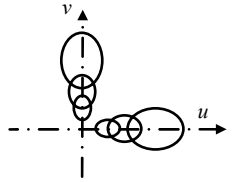

Figure 3: Bank of Gabor filters with 3 scales and 2 orientations

Using complex images can be very helpful, especially when intensity or focus variations occur. Intensity variations will be visible in the magnitude image, and will affect the features produced by Gabor analysis of the magnitude image. Nonetheless it will not affect the phase image that only reflects the geometrical structure of the texture. Thus, features produced by a Gabor analysis on the complex image will not be as sensitive to intensity variation, and will provide a more uniform response. Focus changes are very obvious on the magnitude image, and dramatically change the features produced by Gabor filtering. The complex image is not as sensitive to focus changes if they stay within the wavelength depth, because part of the 3D information will still overlap between two different focus levels. Thus, the features produced by Gabor filtering on complex images are almost invariant to focus variations. For this study, we compared several algorithms to take better advantage of the complex information contained in the images.

3.1. Normalized amplitude image

In this case, the phase of the signal is discarded, and the amplitude of the image $A(x,y)$ is normalized by dividing each pixel by the sum of the mean and the standard deviation values in an L×K sliding window (we usually set L=K=5). This case is used as a reference of the performances of the Gabor filtering on a real image.

$$A_N(x,y) = \frac{A(x,y)}{\mu_{L\times K}(x,y) + \sigma_{L\times K}(x,y)}. \tag{6}$$

3.2. Phase image

The phase image $I_\varphi(x,y)$ is obtained by dividing the complex image $I(x,y)$ by the amplitude $A(x,y)$ of $I(x,y)$. This is practically done by dividing the real and imaginary part of the image by the amplitude.

$$I_\varphi(x,y) = \frac{I(x,y)}{A(x,y)} = e^{j\varphi(x,y)}. \tag{7}$$

We can evaluate the importance of the phase information on the image when no amplitude information is available and see its relevance for segmentation work. Since we get a complex image, it can be directly transformed into Fourier space to be filtered by Gabor filters so that we do not have to deal with phase unwrapping.

3.3. Complex image

The complex image $I(x,y)$ is transformed in the Fourier space and directly used as input for the Gabor filters.

3.4. Complex image with normalized amplitude

In this case, we recreate a complex image $I_N(x,y)$ as a combination of the normalized amplitude image $A_N(x,y)$, and the phase image $I_\varphi(x,y)$.

$$I_N(x,y) = I_\varphi(x,y)\cdot A_N(x,y) = \frac{I(x,y)}{A(x,y)}\cdot A_N(x,y). \tag{8}$$

4. RESULTS

The segmentation tests were performed on a memory wafer, where 3 different areas were required to be segmented. These areas are as follows:

- DRAM area which is a fine regular texture that shows a lot of process variations
- Logic area which is a composite of coarse textures
- Blank area which does not contain any structure

To include a maximum contrast variation, we scanned a column of 1728 images taken across an entire wafer, and covering 24 dies. Fifteen sets of training samples are selected within the column, to cover the whole range of fluctuations. For each training set, a single image is used to extract training samples of each type of texture. This way, we can evaluate the classifier performances when a single image is used to train it. This operation is performed with each training set, and each set of features, to identify the best set of feature when using a single image to train the classifier.

Each image is 436 by 436 pixels, and the segmentation is performed pixelwise. The segmented images are placed in a mosaic of 24 columns, corresponding to the 24 dies. The segmentation is performed using the SVM classifier [7], with an RBF kernel. The classifier's

parameters (C, γ) = (20, 0.5) are set using a five fold cross-validation.

The table 1 presents the average misclassification rate for the fifteen segmentations, corresponding to the fifteen training sets. The results show the importance of the phase information for the segmentation task, since the best results are achieved when the phase is involved. The wavelet transform, and Gabor filters on the normalized amplitude images give overall good results; however, the boundaries between two different textures are not very well resolved, with a smearing of the decode bars area over the DRAM area, and the features are correlated with the contrast variation, which causes the features of different classes to overlap. Therefore, few places of the DRAM area are classified as decode bars. Using Gabor on phase images gives good results, especially with a good segmentation at the boundary between different textures. There are only a few places where we can see some misclassification in the DRAM area. Using Gabor on complex images gives also good results at the boundaries. However, since the amplitude image is not normalized, illumination variations from one field of view are not corrected, which creates misclassifications in the images that are over or under-exposed compared to the image used for the training. Using Gabor on complex images with normalized amplitude images gives the best results, with a very good segmentation at the boundaries. The combination of the phase information with the corrected amplitude generates a set of features that is highly immune to variations, since we can get an accurate segmentation with each training set.

Filtering method	*Average Misclassification Rate*
Wavelets on normalized amplitude images	***4.82%***
Gabor on normalized amplitude images	***6.20%***
Gabor on phase images	***4.46%***
Gabor on complex images	***10.62%***
Gabor on complex image with normalized amplitude images	***4.09%***

Table 1. Average misclassification rate on the segmentation

4. CONCLUSION

In wafer inspection, the performance of segmentation is critical since the misclassification of an area can create a false detection, or increase the overall noise level in the area, that would result in a higher threshold with the risk of missing a critical defect. Therefore, it is crucial to reach an optimal performance, and also to require a minimal input from the operator to increase the productivity of the tool. We previously developed a technique designed to train the classifier with a small set of training samples. The work can be applied to any type of wafer inspection optical tool, but in the particular case of the DDH tool, the extra information provided by the complex nature of the image can be used to improve our previous work. The phase information shows a strong invariance to non uniformities and can readily be used for image segmentation.

5. REFERENCES

[1] C. E. Thomas Jr., et Al. "Direct to digital holography for high aspect ratio inspection of semiconductor wafers.", *2003 International Conference on Characterization and Metrology for ULSI Technology, Proc. AIP v. 683*, Austin, pp. 254-270, March 2003.

[2] P. Bourgeat, F. Meriaudeau, P. Gorria, K.W. Tobin, "Content-based segmentation of patterned wafer for automatic threshold determination", *Proc. SPIE*, *Vol. 5011*, Santa Clara, pp. 183-189, January 2003.

[3] P. Bourgeat, F. Meriaudeau, K.W. Tobin, P. Gorria, "Patterned wafer segmentation", *Quality Control by Artificial Vision*, *Proc. SPIE v. 5132*, Gatlinburg, pp. 36-44, May 2003.

[4] K.W. Tobin, "Inspection in Semiconductor Manufacturing", *Webster's Encyclopedia of Electrical and Electronic Engineering*, vol. 10, pp. 242-262, Wiley & Sons, NY, NY, 1999.

[5] P. Dutilleux "An Implementation of the algorithme à trous to compute the wavelet transform", in Wavelets: Time Frequency Methods and Phase Space. Berlin: Springer IPTI, pp 298-304, 1989.

[6] J. Miteran, P. Gorria, M. Robert, "Classification géométrique par polytopes de contraintes. Performances et intégration", Traitement du Signal, vol. 11, n°5, pp 393-408, 1994.

[7] V.N. Vapnik, "The nature of statistical learning theory". New York: Springer Verlag, 1995.

[8] H.A. Zebker, Y. Lu, "Phase unwrapping algorithms for radar interferometry: residue-cut, least-squares, and synthesis algorithms" JOSA A, Vol. 15 Issue 3 pp. 586, March 1998.

[9] C.T. Allen, "Interferometric synthetic aperture radar", IEEE Geoscience and Remote Sensing Society Newsletter, No. 96, pp. 6-13, Sept. 1995.

[10] A.C. Bovik, M. Clark, W.S. Geisler, "Multichannel texture analysis using localized spatial filters", IEEE Trans. Pattern Anal. Machine Intell., vol. 12, no. 1, pp. 55-73, Jan. 1990.

[11] S.E. Grigorescu, N. Petkov, P. Kruizinga, "Comparison of texture features based on Gabor filters", IEEE Trans. on Image Proc., vol. 11, no. 10, pp 1160-1167, Oct. 2002.